Physical and hydraulic response of geomembrane wrinkles underlying saturated fine tailings

P. Joshi[1], R. K. Rowe[2] and R. W. I. Brachman[3]

[1]*Laboratory Specialist, Golder Associates Ltd. Mississauga, Ontario, Canada, L5N 7K2, E-mail: prabeen_joshi@golder.com*
[2]*Professor and Canada Research Chair in Geotechnical and Geoenvironmental Engineering, GeoEngineering Centre at Queen's – RMC, Queen's University, Kingston, Canada, K7L 3N6, E-mail: kerry.rowe@queensu.ca (corresponding author)*
[3]*Professor, GeoEngineering Centre at Queen's – RMC, Queen's University, Kingston, Canada, K7L 3N6, E-mail: brachman@queensu.ca*

Received 13 March 2016, revised 25 June 2016, accepted 26 June 2016

ABSTRACT: The effect of applied pressure on the deformation of a prescribed wrinkle, with and without a hole, in four different geomembranes (1 and 2 mm thick high density polyethylene and 1 and 2 mm thick linear low density polyethylene), placed on a compacted silty-sand underliner and backfilled with saturated fine tailings at 65% solids content, is investigated. For the 1 mm thick geomembranes without holes, the gap beneath the wrinkle was eliminated (but the geomembrane was excessively strained) at an applied total stress of 250 kPa, whereas for the 2 mm thick geomembranes the gap remained even under a total stress of 1000 kPa. The short-term performance was the same for both LLDPE and HDPE. For wrinkles with a hole, any gap that remained beneath the wrinkle was completely filled by tailings. The tailings migrated into the gap beneath the wrinkle partly as free-flowing slurry and partly under the applied hydraulic gradient. There was a difference in the shape of the final wrinkle depending on whether the hole in the wrinkle was present before or after backfilling with tailings. However, the same leakage was measured through a 10 mm diameter hole in both cases. With an increase in applied vertical stress, the leakage decreased.

KEYWORDS: Geosynthetics, Geomembrane, Holes, Leakage, Tailings

REFERENCE: Joshi, P., Rowe, R. K. and Brachman, R. W. I. (2016). Physical and hydraulic response of geomembrane wrinkles underlying saturated fine tailings. *Geosynthetics International*. [http://dx.doi.org/10.1680/jgein.16.00017]

1. INTRODUCTION

Geomembranes used in mining applications are most commonly either made from high-density polyethylene (HDPE) or linear low-density polyethylene (LLDPE) (Rowe *et al*. 2013). Typically, the geomembranes are 1.0 to 2.5 mm thick and are used, either as a single liner or as a component of a composite liner system, to minimise both advective and, for inorganic contaminants, diffusive transport. With these geomembranes, the leakage (fluid flow under a hydraulic gradient) is effectively limited to flow through holes in the geomembrane that most commonly arise either during construction (including during placement of material over the geomembrane) or subsequently due to stress cracking (Rowe *et al.* 2004; Rowe 2012). It is often assumed that a geomembrane installed with good construction quality assurance (CQA) will have 2.5–5 holes per hectare (Giroud and Bonaparte 1989a, 1989b, 2001). The number of holes may be substantially higher with poor CQA or if the geomembrane is in contact with an underliner (foundation) containing gravel and/or is overlain by a coarse (gravel) backfill (e.g., drainage layer) without adequate geomembrane protection (Rowe *et al*. 2013; Brachman *et al*. 2014). On the other hand, with good CQA, a well-graded smooth foundation and a suitable overlying protection layer, short- and long-term damage to the geomembrane can be kept to a very low level (Saathoff and Sehrbrock 1994; Tognon *et al*. 2000; Gudina and Brachman 2006; Brachman and Gudina 2008; Dickinson and Brachman 2008; Rowe *et al*. 2013; Brachman *et al*. 2014).

Leakage through a geomembrane will depend on: the number and size of holes; the thickness and hydraulic conductivity of the soils in contact with the geomembrane; the hydraulic gradient across the liner; the interface transmissivity between the geomembrane and the adjacent soil; and wrinkles (waves) in the liner (Giroud 1997; Rowe 1998, 2012; Rowe *et al.* 2004).

Wrinkles are either caused by irregularities (e.g., due to geometry such as corners or to poor placement) or in-plane thermal expansion caused by the rise in geomembrane surface temperature after the geomembrane is welded (Pelte *et al*. 1994; Take *et al*. 2012). Wrinkling causes a loss of intimate contact between the geomembrane and underlying soil layer (Rowe 1998; Rowe *et al.* 2004). If these wrinkles are buried when fill is placed over the geomembrane and then subjected to overburden pressures, they will experience some reduction in height and width, but a gap remains between the geomembrane and the underlying soil (Stone 1984; Soong and Koerner 1998; Gudina and Brachman 2006; Brachman and Gudina 2008; Take *et al*. 2012). Previous studies have also shown that two or more wrinkles can intersect, forming a network of interconnected wrinkles that increases (i) the total effective length of a wrinkle; (ii) the probability of a hole coinciding with a wrinkle in the interconnected wrinkle network; and (iii) leakage through the liner. For example, Chappel *et al*. (2012a) conducted a field study to quantify the effective length of connected wrinkles at different times of the day, and reported that on the flat base portion of a municipal solid waste (MSW) landfill the maximum connected length was 6600 m/ha at 13:45 on a hot day in June. For a wrinkle network of this magnitude, Rowe's (Rowe 1998) equation gives a flow of over 1000 litres per day per hectare (lpdh) when the hole size is sufficient that it does not limit the flow and there is an underlying geosynthetic clay liner (GCL) with hydraulic conductivity, $k = 2 \times 10^{-10}$ m/s, thickness, $t = 0.01$ m, interface transmissivity between the geomembrane and GCL, $\theta = 2 \times 10^{-10}$ m^2/s, and head difference, $h = 0.3$ m.

Prior to this present study, little was known about the potential leakage through a hole in a geomembrane wrinkle in a tailings storage facility, since knowledge from the landfill configuration cannot be transferred to a tailings configuration due to the substantial differences in the nature of the underlying and overlying materials (Figure 1) and, consequently, the stresses transferred to the geomembrane wrinkle. Modern landfills commonly have a 0.3 m thick gravel drainage layer above the geomembrane liner (Figure 1a). With the leachate head generally regulated at ≤ 0.3 m, the vertical effective stress acting on top of the liner is generally very close to the total stresses due to the overlying waste. At the geomembrane wrinkle, due to the deformation of the relatively flexible wrinkle under an applied stress, arching may be induced in the interlocking gravel particles (Terzaghi *et al*. 1996) thereby reducing the stresses transferred to the wrinkle (especially horizontally). Whereas, in a tailings storage facility, it is reasonable to assume that saturated tailings with a low solids content and initially very low shear stiffness apply isotropic or near isotropic stresses to the wrinkle surface (Figure 1b). In addition to that, there is a possibility that any gap present within the wrinkle may be filled with free-flowing tailings if there is a hole coincident with the wrinkle. However, it is presently not known how the physical and hydraulic performance of geomembrane wrinkles at the base of a tailings containment facility would be influenced by the combined effect of (i) the hydraulic properties of the overlying tailings; (ii) stress distribution on the geomembrane wrinkle; and (iii) the presence of free-flowing tailings adjacent to the geomembrane.

The objective of this study is to provide the first insight into the short-term physical response of geomembrane wrinkles under simulated tailings containment facility conditions. The influence on wrinkle deformation of the type and thickness of the geomembrane, backfill, applied total vertical stress and pore pressure are examined. Additionally, the effect of tailings migration through a 10 mm diameter hole into the gap beneath the geomembrane wrinkle on wrinkle deformation and leakage through the hole are also studied.

2. EXPERIMENTAL DETAILS

2.1. Apparatus and boundary conditions

The experiments performed in this study were conducted in a rigid cylindrical steel test cell with an inside diameter of 590 mm, height of 500 mm, 7 mm thick side walls and 50 mm thick top and bottom caps (Figure 2). A total vertical pressure of up to 1000 kPa could be applied by introducing fluid pressure on top of a rubber bladder secured tightly between the lid and the body of the test cell. Horizontal stresses corresponding to essentially zero lateral strain conditions develop due to the rigidity of the cell limiting outward deflection. Pore pressures were applied by injecting water at a controlled pressure

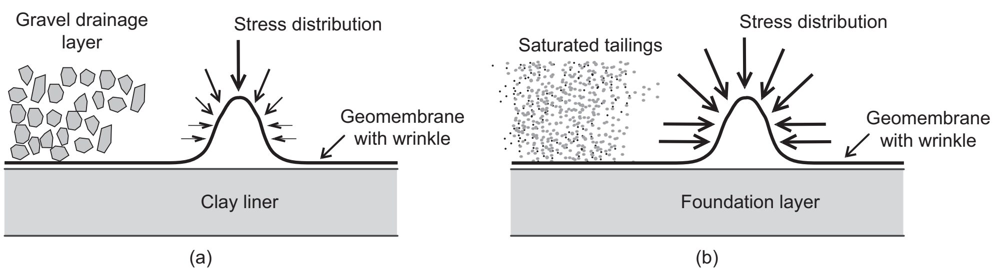

Figure 1. Stress distribution: (a) on the surface of a geomembrane wrinkle covered by a gravel drainage layer in a municipal solid waste landfill configuration. The magnitude of the horizontal component of the stresses is smaller than the vertical component due to interlocking of gravel particles and positive arching, (b) on the surface of a geomembrane wrinkle in a mine tailings containment configuration. The vertical and horizontal components of the applied stresses are equal due to isotropic or near-isotropic conditions

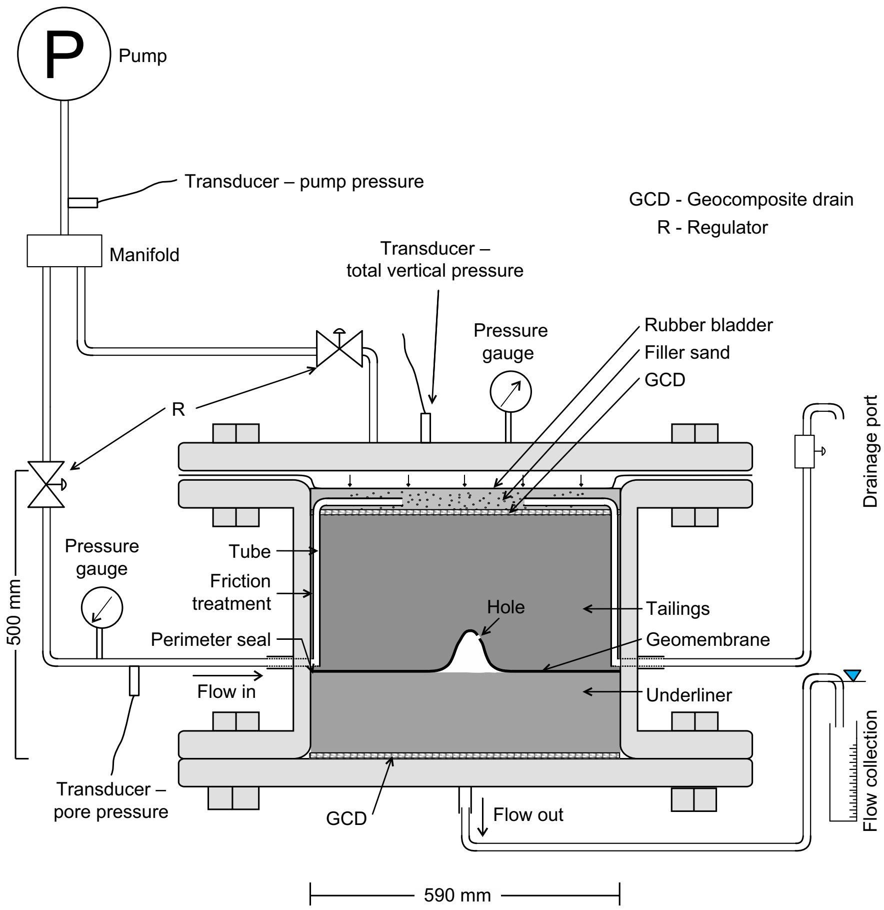

Figure 2. Cross-section of the test apparatus and test configurations

between two geocomposite drains (GCDs) placed on top of the tailings. A GCD was also placed at the bottom of the cell, above the steel bottom, to conduct water to the drainage outlet and provide a known bottom boundary pressure head. The cell wall provided a radial no-flow boundary. Friction along the inner wall surface was reduced by using two layers of 0.1 mm thick polyethylene sheets, with a special lubricant between them allowing the outer layer to slip with very little resistance as the soil in the cell consolidates and compresses. Tognon *et al.* (1999) showed that the boundary friction is reduced to less than 5° with this arrangement.

2.2. Materials and test procedure

The key index properties of the four geomembranes examined in the study (1 and 2 mm thick LLDPE and HDPE) are given in Table 1. The stiffness index, κ, defined here as the ratio of yield strength to yield strain for each geomembrane, was calculated (Table 1). The stiffness index was then normalised with respect to the value for the least stiff (i.e., the 1 mm thick LLDPE) geomembrane to give a value, Ω (Table 1) which is the relative tensile stiffness of that geomembrane compared to the 1 mm thick LLDPE used in this study. For example, $\Omega = 3.4$ and 3.9 for a 2 mm thick HDPE in machine and cross-machine direction implies that the 2 mm thick HDPE is 3.4 times stiffer than the 1 mm thick LLDPE geomembrane in the machine direction and 3.9 times stiffer in the cross-machine direction. A geomembrane with higher Ω value is expected to provide greater resistance to wrinkle deformation if subjected to similar stresses by a given surcharge. In addition to the values for the geomembranes examined in this study, the corresponding values for a 1.5 mm thick HDPE geomembrane used by the previous researchers in a landfill configuration is also included for comparison (Table 1), and is discussed later.

In all experiments, a 0.14 m thick silty-sand base underliner ($d_{50} = 0.19$ mm, $d_{10} = 0.06$ mm, $C_u = 7.3$, $C_c = 3.4$) was compacted at a dry density of 1650 kg/m^3 at 10.6% gravimetric water content. The silty-sand had approximately 12% non-plastic fines (< 75 μm) with less than 1% clay size (< 2 μm) and a hydraulic conductivity, k, of 3.6×10^{-6} m/s at an effective stress $p' = 500$ kPa (total stress $p = 600$ kPa, pore pressure $u = 100$ kPa). Once placed, this underliner was saturated from the bottom.

A geomembrane with a prescribed wrinkle was placed on the saturated underliner (Figures 2 and 3). As placed, the geomembrane wrinkle was 60 mm high and 200 mm wide (Figure 4). These dimensions were selected to be within the range reported based on field observations for 1.5 and 2 mm thick HDPE geomembranes (Pelte *et al.* 1994; Rowe *et al.* 2012; Chappel *et al.* 2012b). A bentonite-based perimeter seal was applied on the top and bottom of the geomembrane edges around the circumference to limit any preferential flow (Figure 2).

Table 1. Index of stress-strain properties (measured in machine (MD) and cross-machine (X-MD) direction) of the HDPE and LLDPE geomembranes studied (tested according to ASTM D6693)

GMB type	Thickness (mm)	Yield strength (kN/m)		Elongation at yield (%)		Yield strain		Break strength (kN/m)		Elongation at break (%)		Yield strength ÷ yield strain (kN/m) (κ)		$\kappa_{GMB} \div \kappa_{1\ mm\ LLDPE}$ (Ω)	
		MD	X-MD	MD	X-MD	MD	X-MD	MD	X-MD	MD	X-MD	MD	X-MD	MD	X-MD
LLDPE	1	12.2 ± 0.2	11.8 ± 0.3	22.4 ± 1.8	21.9 ± 1.2	0.22	0.22	35.7 ± 2.7	34.6 ± 2.8	1238 ± 96	1161 ± 130	54	54	1.0	1.0
	2[a]	30.9 ± 0.4	31.1 ± 0.5	21.2 ± 0.6	21.5 ± 0.6	0.21	0.21	68.5 ± 4	67.1 ± 6.4	920 ± 62	960 ± 104	146	145	2.7	2.7
HDPE[b]	1	18.3 ± 0.4	20.7 ± 1.0	24.7 ± 0.9	19.0 ± 1.2	0.25	0.19	34.1 ± 0.9	35.3 ± 0.9	784 ± 14	852 ± 37	74	109	1.4	2.0
	2	37.2 ± 1.3	38.4 ± 0.8	20.0 ± 0.4	18.4 ± 0.6	0.20	0.18	65.6 ± 4.1	66.0 ± 3.2	830 ± 38	854 ± 33	186	208	3.4	3.9
HDPE	1.5[c]	28.9 ± 1	30.8 ± 0.4	22.1 ± 0.8	17.7 ± 0.44	0.22	0.18	47.3 ± 1.8	46.8 ± 1.8	821.8 ± 30	874 ± 46	131	175	2.4	3.2

[a]Ramy Awad (personal communication); [b]Amr Ewais (personal communication); [c]Abdelaal *et al.* (2012).

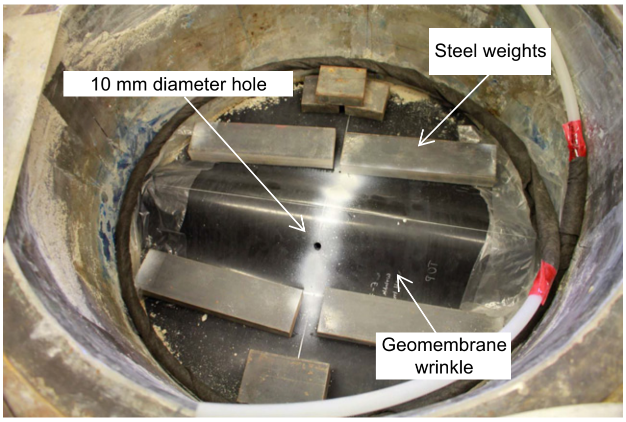

Figure 3. An artificially formed geomembrane wrinkle (200 mm wide and 60 mm high) with a 10 mm diameter hole on the top side (1 mm thick LLDPE; test W1). Steel weights were used to form the shape of the wrinkle and these were removed during backfilling

Several prototype tests (not reported in this paper) suggested that a wrinkle in the 1 mm thick geomembrane without any holes may deform to an extent that the inner sides of the wrinkle would come in contact with each other at 250 kPa applied vertical stress. To provide documentary evidence of any such contact, one of the inner sides of the wrinkle was painted white and a grid in black ink was placed on the other side (Figure 5a) such that upon contact, the ink mark would transfer to the white paint (Figures 5b and 5c). A double-sided adhesive tape was also attached on the side with the paint in order to preserve the shape of the compressed wrinkle during the post-test observation (Figures 5a and 5b). Although deformations of 2 mm thick geomembrane wrinkles were not expected to be as large as in 1 mm thick geomembranes, white paint, ink marks and double-sided adhesive tape were applied for consistency.

In all tests, except test W3, a 10 mm diameter hole was introduced to study leakage and/or tailings migration into the gap beneath the wrinkle. The hole diameter was selected based on the survey conducted by Colucci and Lavagnolo 1995, where the selected hole diameter represented the median area of defects found in geomembrane liners. While the hole size remained the same in all tests, the tests differed in terms of the time of introduction of the hole. For tests W1 (with 1 mm-thick LLDPE) and W5 (with 2 mm thick LLDPE), the hole was introduced in the geomembrane wrinkle prior to the placement of tailings slurry to simulate field conditions where holes were formed and went undetected prior to backfilling. For tests W2 (with 1 mm thick LLDPE) and W4 (with 1 mm thick HDPE), the hole was drilled in the wrinkle after the tailings slurry had been consolidated at 250 kPa for 100 h to simulate field conditions where a hole was formed after backfilling and consolidation of tailings.

A 300 mm thick layer of tailings ($d_{50} = 0.19$ mm, $d_{10} = 0.014$ mm, $C_u = 18.4$ and $C_c = 2.9$) as a slurry with 65% solids content by mass was placed on top of the geomembrane layer at a bulk density of 1780 kg/m^3.

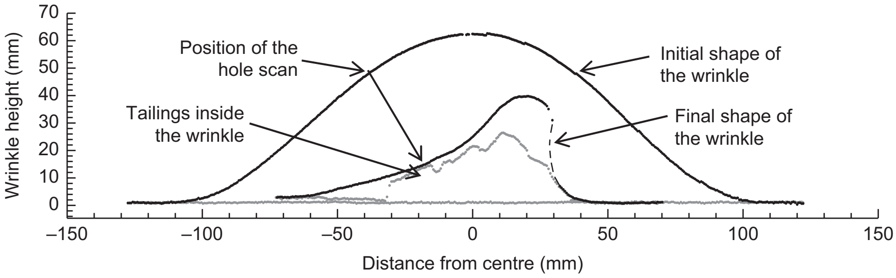

Figure 4. Cross-section showing the initial and final shape of the wrinkle with tailings partially filling the gap beneath the wrinkle (test W1). The wrinkle was covered with 300 mm tailings slurry (with 65% solids) and left for 24 h

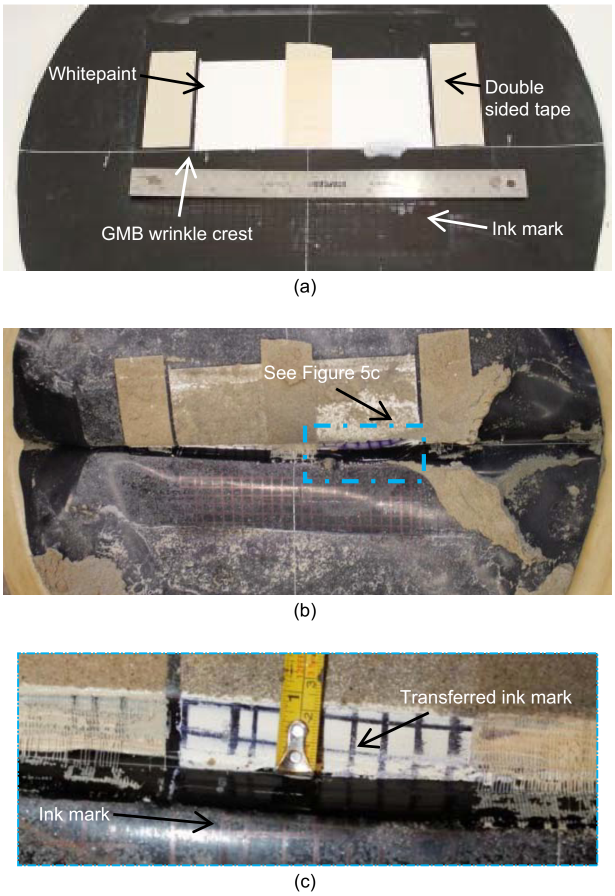

Figure 5. Underside of the 1 mm thick LLDPE geomembrane: (a) before test W2, with white paint on one side of the wrinkle crest line and ink marks on the opposite side. A double-sided tape is attached on one side to prevent the geomembrane from relaxing after the applied stress is removed, (b) post-test photograph showing the underside after the termination of test W2, (c) is an enlarged view of the inset in Figure 5b showing the ink marks transferred from one side of the wrinkle to the white paint on the opposite side, confirming contact between the inner sides of the wrinkle

The tailings had approximately 27% non-plastic fines with less than 3% clay size fraction and a hydraulic conductivity of 5.4×10^{-7} m/s at an effective stress of 50 kPa (total stress $p = 150$ kPa, pore pressure $u = 100$ kPa) and 4.2×10^{-7} m/s at effective stress of 500 kPa ($p = 600$ kPa, $u = 100$ kPa). The same tailings were used in all tests.

Above the tailings, two layers of geocomposite drains, a 30 mm thick leveling sand layer and a rubber bladder was placed to complete the test setup (see Figure 2). The geocomposite is where the pore pressure was applied along the top surface of the tailings, while the rubber bladder was used to apply the total vertical pressure. Once all the materials were placed in the cell, vertical pressures were applied in 50 kPa increments every 10 min to reach 250 kPa, which was then held constant for 100 h (with the exception of tests W1 and W5, as discussed later). The excess pore pressure generated in the tailings and underliner, due to the increase in total stress, was allowed to dissipate from the drainage port on the side of the test cell and flow collection ports at the bottom of the cell respectively (Figure 2). After 100 h, the extent of wrinkle deformation was quantified (Table 2) through a narrow vertical observation trench excavated for this purpose (Figure 6). After making the observations, the tailings removed from the trench were re-packed into the trench at 25% moisture content and the tailings was re-consolidated at 250 kPa for another 100 h prior to starting the permeation phase of the experiment.

Tests W2, W4 and W5, were permeated at a combination of different applied pressures to simulate a tailings storage facility at various stages of development. The first combination approximates a thickness of tailings applying a total stress of $p = 250$ kPa on the lower 0.3 m of tailings, where the tailings are submerged under sufficient water to generate a pore pressure in the lower 0.3 m of tailings of $u = 200$ kPa, giving an effective stress $p' = 50$ kPa in the lower 0.3 m of tailings. Considering the stresses in the same lower 0.3 m of tailings, the second stress combination had tailings applying $p = 1000$ kPa, water ponding on the tailings yielding $u = 500$ kPa and $p' = 500$ kPa in the lower 0.3 m of tailings (Figures 7a–7c).

Permeation tests were terminated after reaching steady-state flow (e.g., Figure 7d). In all tests, a narrow vertical observation trench at the centre of the cell was excavated through the tailings to acquire the final deformed shape of the geomembrane wrinkle using a line laser profiler (Figure 6).

3. RESULTS

The base underliner, the tailings and hole size (if present) were kept the same in all experiments so that the effect of

Table 2. Initial and final wrinkle dimensions of geomembrane wrinkles subjected to different stresses

Test	Geomembrane thickness and type	Initial wrinkle dimensions (mm)		Test conditions (kPa)			Final wrinkle dimensions (mm)	
		Height	Width	Total stress	Pore pressure[a]	Effective stress[a]	Height	Width
W1	1 mm LLDPE	60	200	~6	–	~6	40	100
W2	1 mm LLDPE			250	0	250	27	20
W3	1 mm HDPE			250	0	250	26	38
W4	2 mm HDPE			250	0	250	40	80
				1000	500	500	38	70
W5	2 mm LLDPE			1000	500	500	35[b]	67[b]

[a]At the top of the tailings; the pore pressure below the hole is about 1–1.5 kPa and the effective stress in the tailings above the hole will be substantially higher than at the top due to seepage forces.
[b]The reported dimensions are for the central big wrinkle only (see Figure 11). Height measured from the top of the foundation.

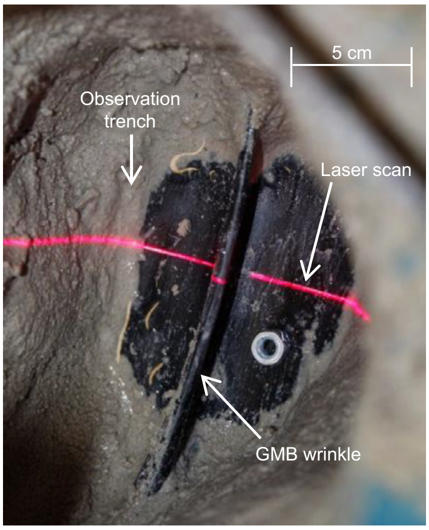

Figure 6. Photograph showing the deformed geomembrane wrinkle being profiled using a line laser through a vertical observation trench. The 1 mm thick HDPE geomembrane wrinkle was allowed to deform under 250 kPa overburden stress for 100 h (test W3)

geomembrane type and thickness, applied total stress, applied pore pressure and time of hole placement could be explored. These variables are discussed below.

3.1. Physical response of geomembrane wrinkles under applied vertical stresses

3.1.1. *1 mm thick geomembranes*
A 1 mm thick LLDPE geomembrane wrinkle with a 10 mm diameter hole on the side (Figure 3; test W1) was covered with 300 mm thick tailings slurry at 65% solids content (applying approximately 6 kPa of total vertical stress) and left for 24 h without any externally applied load. A cross-section of the initial and deformed shape of the geomembrane (Figure 4) shows that the wrinkle height and width were reduced to 67% (40 mm) and 50% (100 mm) of their original values. The final wrinkle was non-symmetrical, and skewed away from the side where the hole was placed. The wrinkle possibly skewed because the tailings that entered through the hole first resisted any additional lateral stress (due to the increasing depth of tailings) on the side with the hole, and allowed the other side to cave in. It is not known whether the same would happen for tailings with lower solids content, however it can be anticipated that tailings with lower solids would flow even more easily through the hole into the gap beneath the wrinkle than the tailings slurry tested.

Experiments were conducted using a 1 mm thick LLDPE (test W2) and HDPE (test W3) geomembrane with a wrinkle (but without a hole) to investigate the effect of larger applied stress on the geomembrane wrinkle, initially without tailings intrusion into the wrinkle. In test W2, the hole was added after the tailings slurry had been consolidated at 250 kPa for 100 h to simulate field conditions where a hole was formed after backfilling and consolidation of tailings (discussed in detail later). Test W3 was terminated after evaluating wrinkle deformation. The final shape of the wrinkle when subjected to a total vertical pressure of 250 kPa for 100 h for otherwise the same test conditions as in test W1 are shown in Figure 8. Post-test observation revealed that the inner sides of the wrinkle were squeezed together to give a near vertical projection. The geomembrane wrinkle deformation resulted in a very high curvature on the crest and toe of the wrinkle, where there were large strains that could, in the long term, cause stress cracking (e.g., Abdelaal *et al*. 2013; Ewais *et al*. 2014). Inspection of the underside of both geomembrane wrinkles provided further evidence of contact, as the ink marks were found to have transferred onto the side with the paint (Figures 5b and 5c). Figure 9 shows a photograph of the deformed 1 mm thick LLDPE wrinkle. The final remaining height and width at the base of the 1 mm thick LLDPE wrinkle were 45% (27 mm) and 10% (20 mm) of the initial dimensions, and the height and width at the base of the 1 mm thick HDPE wrinkle were 43% (26 mm) and 19% (38 mm). The larger remaining width in the 1 mm thick HDPE geomembrane wrinkle may be due to its slightly higher stiffness compared to the 1 mm thick LLDPE geomembrane (Table 1).

3.1.2. *2 mm thick geomembranes*
An experiment was conducted with a 2 mm thick HDPE geomembrane wrinkle (test W4), initially without a hole,

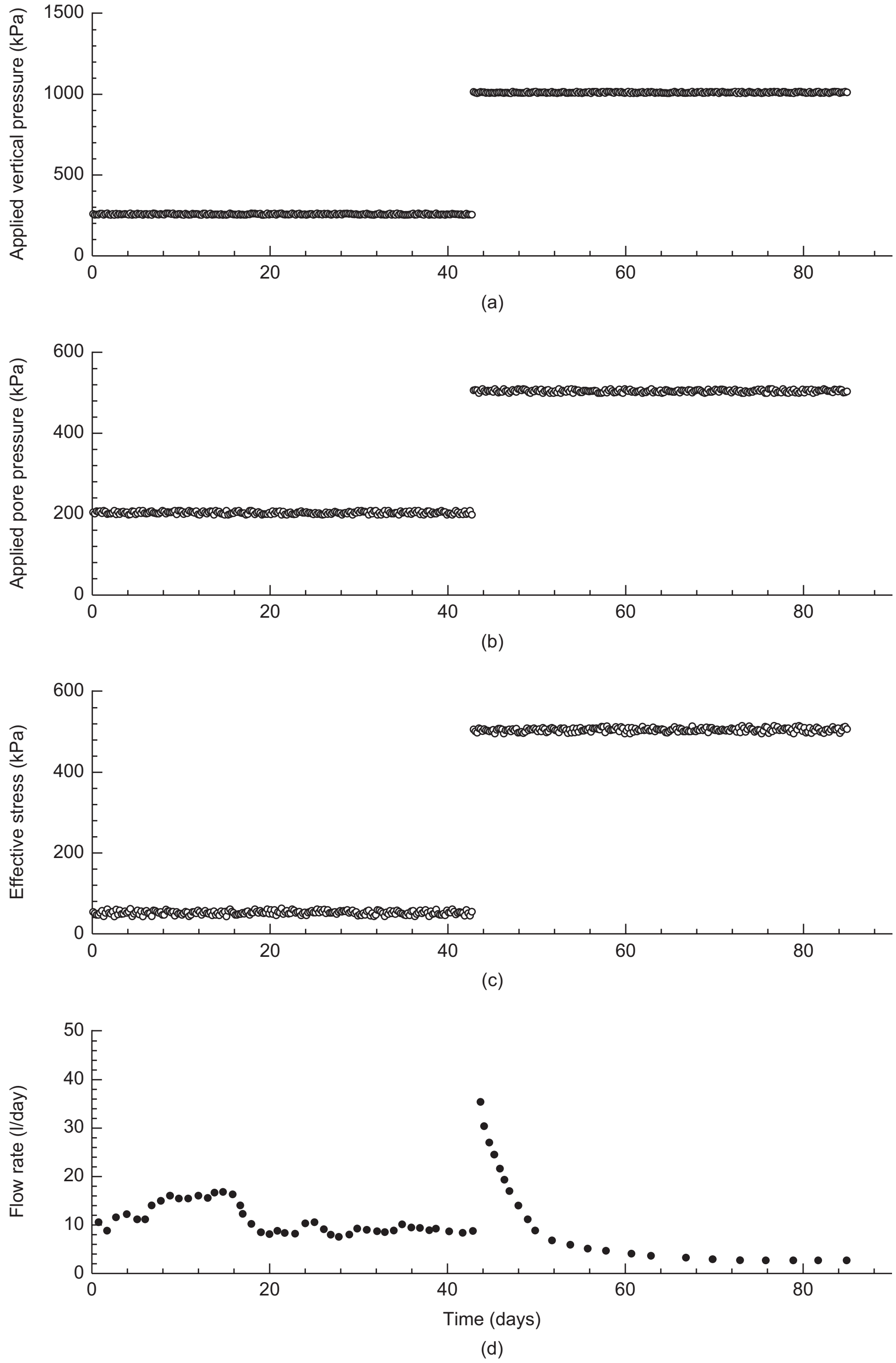

Figure 7. Plots of: (a) applied vertical stress, (b) applied pore pressure, (c) effective stress, and (d) measured flow versus time for test W4

subjected to same conditions as in test W3 with a 1 mm thick HDPE geomembrane wrinkle and a total stress of 250 kPa sustained for 100 h. After 100 h, the height and width of the wrinkle were reduced to 67% (40 mm) and 40% (80 mm) of the initial dimensions. The remaining void beneath the 2 mm thick HDPE wrinkle was 1.5 to 2 times larger than that in the 1 mm thick HDPE geomembrane (Figure 10). The larger remaining gap beneath the wrinkle in the 2 mm thick geomembrane is attributed to the thicker geomembrane having greater stiffness, and hence greater resistance to bending along the geomembrane crest line compared to the thinner and less-stiff 1 mm thick geomembranes (Table 1). At a higher applied pressure of $p = 1000$ kPa, $u = 500$ kPa ($p' = 500$ kPa), the wrinkle was reduced to a height and width of 64% (38 mm) and 35% (70 mm), but the gap beneath the wrinkle remained (Figure 11).

Test W5 was conducted with a 2 mm thick LLDPE geomembrane, where a 10 mm diameter hole was placed on the top side of the wrinkle prior to tailings placement so that the tailings slurry could enter the geomembrane wrinkle even before any external stress was applied. As a result, the deformed wrinkle took a different shape to that observed in the 2 mm thick HDPE wrinkle where there was no hole in the wrinkle prior to tailings placement (Figure 11). In addition to the central large wrinkle,

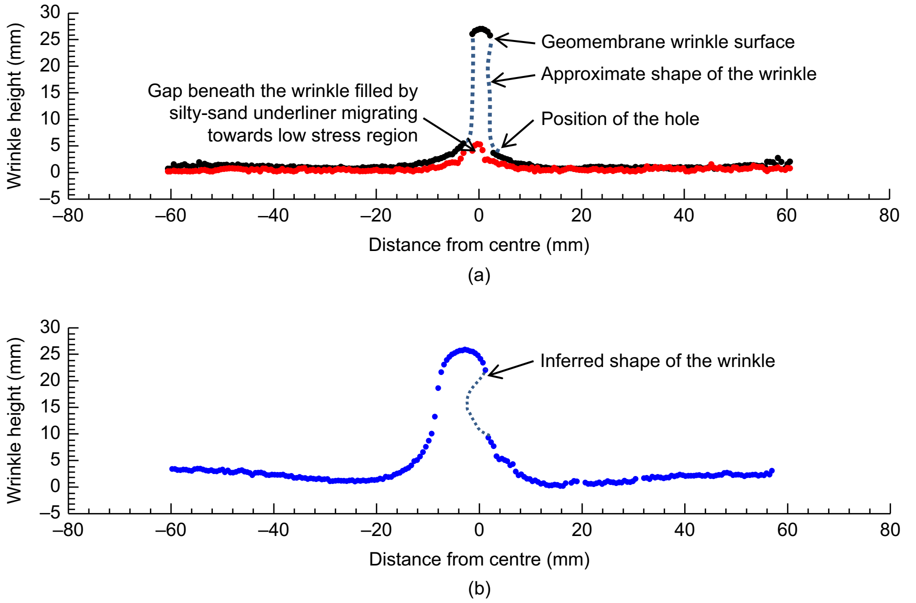

Figure 8. Cross-section through deformed 1 mm thick geomembranes (initially 200 mm wide and 60 mm high) after being subjected to 250 kPa for 100 h. (a) LLDPE wrinkle (test W2), (b) HDPE wrinkle (test W3)

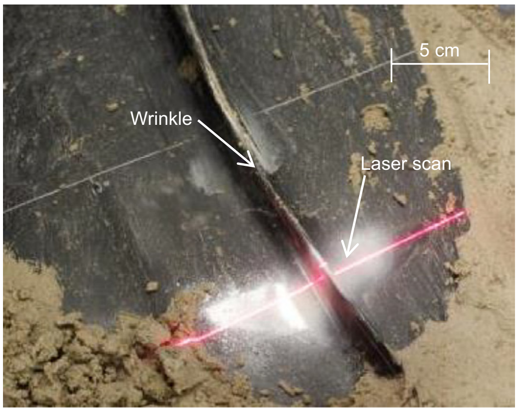

Figure 9. Deformed wrinkle from test W2 after it had been subjected to 250 kPa overburden stress for 100 h. Note that due to the presence of double-sided tape on the inner wall of the geomembrane wrinkle, the sides are still touching even after removal of the stress

there were two other smaller wrinkles on each side of the central wrinkle, introducing multiple locations with higher curvature. These smaller wrinkles caused the final width of the wrinkle to be wider than in the case where no hole was present in the geomembrane wrinkle prior to backfilling. The unique shape of this wrinkle was likely due to the wrinkle deformation occurring only after the gap beneath the wrinkle was partially filled with tailings slurry. The deformed wrinkle was symmetrical at the crest-line, unlike that observed for a less stiff 1 mm thick LLDPE geomembrane in test W1. The final width of the central large wrinkle after being subjected to up to $p = 1000$ kPa and $p' = 500$ kPa was similar to the 2 mm thick HDPE wrinkle in test W4 for same applied stresses. However, the height of the wrinkle was about 3 mm smaller, likely due to the presence of smaller wrinkles that formed on each side of the central large wrinkle.

3.2. Leakage through 10 mm diameter holes on the geomembrane wrinkle

3.2.1. *Hole at the base of the wrinkle after tailings consolidation*

Following a post-consolidation physical evaluation of the wrinkle in the 1 mm thick LLDPE (test W2), a 10 mm diameter hole was drilled at the base of the wrinkle that had been squeezed together, with no gap remaining beneath the wrinkle due to the previously applied pressure (Figure 8a). Tailings that had been removed from the vertical observation trench (at ~21% moisture content) were mixed with water to about 25% moisture content (wet but not free flowing) and packed back into the trench. The permeation test was started after another 100 h of consolidation. The steady-state flow through the hole at $p = 250$ kPa and $u = 200$ kPa ($p' = 50$ kPa) was 2.3 lpd. When the applied stress and pore pressure were increased to $p = 1000$ kPa and $u = 500$ kPa ($p' = 500$ kPa), the flow increased 3.3 fold to 7.6 lpd.

3.2.2. *Hole formed on the top side of the wrinkle after tailings consolidation*

Initially, the 2 mm thick HDPE geomembrane wrinkle in test W4 did not have any hole. After 100 h of sustained vertical pressure of 250 kPa, the stress was removed and an observation trench excavated to allow inspection of the wrinkle (Figure 10). After the inspection, a 10 mm hole was drilled at the top side of the wrinkle (Figure 12). The observation trench was backfilled, and the backfill was consolidated as described for test W2 before starting the permeation phase of the test at $p = 250$ kPa and $u = 200$ kPa ($p' = 50$ kPa; Figure 7). A steady state flow of 8.5 lpd was measured in a permeation test that lasted for 44 days. Although steady state flow conditions were attained in 20 days, the test was allowed to run for twice that time to confirm that a steady state had been reached and that there was no time-dependent effect on flow.

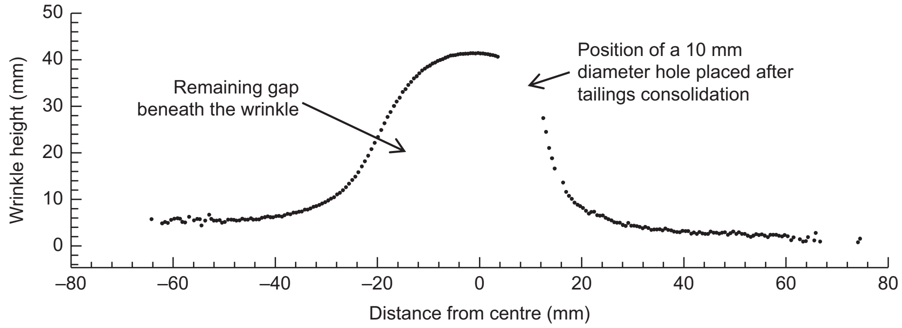

Figure 10. Cross-section through a deformed 2 mm thick HDPE geomembrane wrinkle (initially 200 mm wide and 60 mm high) after being subjected to 250 kPa for 100 h. There is some missing data at the location of the hole because the laser signal was not reflected along the width of the hole

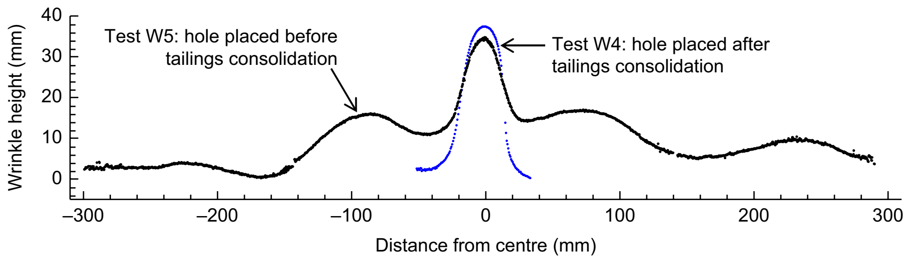

Figure 11. Cross-section through deformed 2 mm GMB wrinkles subjected to a total stress of 1000 kPa. In test W4, the hole was placed after consolidation of tailings under 250 kPa for 100 h. In test W5, the hole was placed before tailings placement. The different shape of the deformed wrinkle in test W5 is due to the gap beneath the wrinkle being partially filled with tailings prior to wrinkle deformation under externally applied stresses

Figure 12. Hole being placed on the top side of the exposed wrinkle (test W4). The wrinkle was painted white to provide a reflecting surface for laser scanning

The test was continued, but at a higher applied stress and pore pressure ($p = 1000$ kPa, $u = 500$ kPa; $p' = 500$ kPa). At first the flow increased, but eventually (26 days after the stress was increased) the steady state flow was at a lower rate of 2.5 lpd (Table 3; Figure 7). This flow, at $p' = 500$ kPa, is about a third of that when the hole was at the base of the wrinkle.

3.2.3. *Hole formed on the top side of the wrinkle prior to backfilling with tailings slurry*

The effect on the flow of having a hole on the geomembrane wrinkle prior to tailings placement was investigated by placing a 10 mm diameter hole on a 2 mm thick LLDPE geomembrane wrinkle prior to backfilling with tailings slurry (test W5). In this test, a total stress of 250 kPa and a pore pressure of 200 kPa (an effective stress of 50 kPa) were applied without a period of tailings pre-consolidation prior to permeation that was permitted in the tests discussed above. The leakage measured at $u = 200$ kPa ($p' = 50$ kPa; $p = 250$ kPa) was 8.4 lpd, and steady-state flow conditions were achieved within 10 days of permeation. At $u = 500$ kPa ($p' = 500$ kPa; $p = 1000$ kPa), flow decreased to 2.6 lpd reaching steady state flow conditions within 11 days of permeation (Table 3).

3.3. Migration of tailings into the wrinkle gap

Migration of tailings into the void beneath the wrinkle was observed to occur in two ways, (i) free flow into the gap beneath the wrinkle through a hole and (ii) flow under a hydraulic gradient (piping).

When the wrinkle (with hole) in a 1 mm thick LLDPE was backfilled with a 300 mm thick layer of free-flowing tailings at 65% solids content and left for 24 h, the gap beneath the wrinkle was partially filled with tailings (test W1). The tailings migrated in and spread out about 6.5 cm laterally into the wrinkle above the foundation sand (Figure 4). The percentage of fines in the tailings inside the wrinkle was the same as in the overlying tailings (27%).

When there was no hole in the 1 mm thick LLDPE wrinkle prior to tailings placement, there was no

Table 3. Summary of permeation tests conducted at 22°C. Materials used in all tests are (a) Silty-sand underliner with ~ 12% fines (passing US sieve #200), (b) Tailings with ~ 27% fines. Initial dimensions of geomembrane wrinkle: 200 mm wide and 60 mm high (see Figure 4). Hole diameter is 10 mm

Test #	Geomembrane thickness and type	Test conditions (kPa)			Time of hole placement	Measured flow (lpd[b])
		Total stress	Pore pressure[a]	Effective stress[a]		
W1	1 mm LLDPE	~ 6	–	~ 6	Before tailings placement	–
W2	1 mm LLDPE	250	200	50	After tailings consolidation	2.3
		1000	500	500		7.6
W3	1 mm HDPE	250	–	250	No hole	–
W4	2 mm HDPE	250	200	50	After tailings consolidation	8.5
		1000	500	500		2.5
W5	2 mm LLDPE	250	200	50	Before tailings placement	8.4
		1000	500	500		2.6

[a]At the top of the tailings; the pore pressure below the hole is about 1–1.5 kPa and the effective stress in the tailings above the hole will be substantially higher than at the top due to seepage forces.
[b]lpd = liters per day.

migration of tailings into the gap beneath the wrinkle (test W2). The void beneath the wrinkle was in fact partially filled with the silty-sand subgrade due to foundation deformation under applied stresses (Figure 8a).

Test W4 examined the effect of the applied hydraulic gradient on tailings migration into the gap beneath the wrinkle in a 2 mm thick HDPE geomembrane. Although the tailings backfill placed after placing a hole on the wrinkle was 75% solids (i.e., not free flowing), post-termination observation of test W4 revealed that the void beneath the wrinkle was entirely filled with tailings (Figure 13a). This implies that, in this case, the tailings mostly migrated under the hydraulic gradient. The tailings migrated laterally up to 15 cm on each side of the centrally located hole. Due to the limited dimensions of the test apparatus and length of tested wrinkle, the extent of potential lateral spreading of tailings into a wrinkle in the field could not be determined.

Similar observations were made in test W5, where the tailings backfill was placed at 65% solids (free-flowing) and there was a hole present in the wrinkle in the 2 mm thick LLDPE geomembrane prior to backfilling. The entire gap beneath the wrinkle was filled with tailings (Figure 13b). It could not be verified if the entire gap was filled with tailings slurry before any pore pressure was applied, or if the gap was partly filled with tailings that migrated under the hydraulic gradient. However, from the final deformed shape of the wrinkle it appeared that the wrinkle deformation happened in at least two stages and that at the time the second deformation occurred, the bottom half of the wrinkle may have already been filled with tailings.

The percentage of fines in the tailings was evaluated at different locations on a vertical plane perpendicular to the geomembrane wrinkle at the centre of the test cell (Figure 14a) for a test with a 2 mm thick HDPE wrinkle (test W4) and one with a 2 mm thick LLDPE wrinkle (test W5; Figure 14b). The percentage of fines inside the wrinkle, close to the hole, was generally higher than at other locations within the wrinkle or above the wrinkle. A slight increase in the fines content of the foundation immediately beneath the wrinkle void was observed.

4. DISCUSSION

If there are no holes in the geomembrane, there will be no significant leakage through the liner. Geomembrane wrinkles are of concern because if there is a hole at the wrinkle there is potential for considerable leakage of fluid through the hole and along the wrinkle network. In a landfill application and others with a highly permeable material above the wrinkle, fluid can have unobstructed access into the gap beneath the wrinkle through a hole. If the pressure head, thicknesses and hydraulic conductivity of the underlying soils, interface transmissivity between the geomembrane and underlying soil, length and width of the wrinkle, and size of the hole in the wrinkle are known, then the leakage can be calculated (Rowe 1998). However, based on this study it appears that the situation is very different with lower permeability and higher compressibility tailings placed over a geomembrane wrinkle.

4.1. Wrinkle deformations

Without a hole, the 1 mm thick geomembrane wrinkles subjected to 250 kPa total stress deformed to an extent that both inner sides of the wrinkle were in contact with each other, with a final remaining height and width at the base of 45% and 10% respectively for 1 mm thick LLDPE and 43% and 19% respectively for 1 mm thick HDPE. Since 1 mm thick geomembranes are not used in the bottom of modern landfills, it is not known with certainty. Whether the same would occur in the presence of a coarse gravel drainage layer. However, it is considered unlikely based on observations for 1.5 mm thick geomembranes in a landfill-based configuration (i.e., with gravel backfill; Figure 1b). For example, for a 1.5 mm thick HDPE geomembrane wrinkle with the same test conditions (initial wrinkle size, $W = 200$ mm and $H = 60$ mm; applied vertical stress = 250 kPa; test

Figure 13. Photographs taken after removing the deformed geomembrane wrinkle followed by termination of the permeation test. (a) after test W4 with a 2 mm HDPE geomembrane where the hole was placed after tailings consolidation (see Figure 12), (b) in test W5 with a 2 mm thick LLDPE geomembrane where the hole was placed before placement of tailings

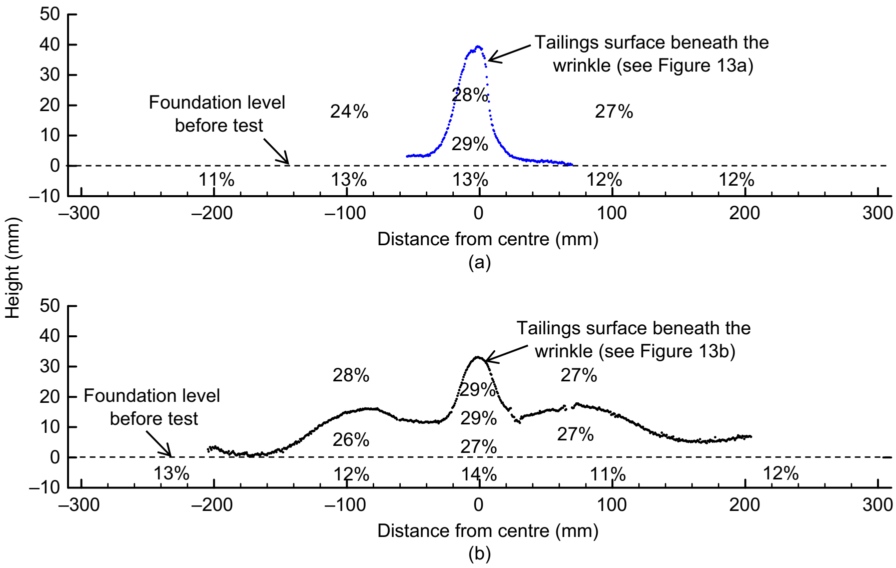

Figure 14. Post-test evaluated percentage fines (passing US sieve #200) from different locations on a vertical plane perpendicular to the geomembrane wrinkle at the centre of the test cell in (a) test W4 with a 2 mm thick HDPE wrinkle, (b) test W5 with a 2 mm thick LLDPE wrinkle

duration = 100 h) but in a landfill-based configuration, Brachman *et al.* (2011) reported a final remaining wrinkle with a height and width of 66% and 45% respectively. In this study, the remaining final height and width of stiffer 2 mm thick HDPE geomembranes were $H = 67\%$ and $W = 40\%$, which is smaller than those reported by Brachman *et al.* (2011) for a 1.5 mm thick HDPE geomembrane.

Although the comparison is not straightforward for wrinkles with two different geomembrane thicknesses and buried beneath different backfills, it is considered likely that a larger lateral stress is applied on the wrinkle surface in a tailings configuration than in a landfill with a gravel drainage layer. This would give rise to larger wrinkle deformations in contact with tailings slurry for a geomembrane with the same thickness and without a hole. The larger wrinkle deformations and smaller remaining wrinkle would be expected to reduce leakage through a given hole in the wrinkle.

4.2. Leakage through a hole in the wrinkle

When a hole was positioned at the base of a wrinkle in a 1 mm thick LLDPE, the leakage was 7.6 liters per day per hole at $p = 1000$ kPa, $u = 500$ kPa at 0.3 m above the liner ($p' = 500$ kPa; test W2). With 5 such holes per hectare, the leakage could be 40 liters per hectare per day (lphd) under these conditions. However, this is a relatively small amount of leakage, and considers a worst case where there is no head loss in the tailings until 0.3 m above the liner. The highest measured flow in this study (8.5 lpd) was for a 2 mm thick geomembrane with a hole on the top side of the wrinkle at $p = 250$ kPa and $u = 200$ kPa ($p' = 50$ kPa). Assuming 5 such holes per hectare, the flow would be a still relatively small 42.5 lpd. This is substantially smaller than that calculated by Rowe (2012) for a pond lined only with a 0.6 m thick compacted clay liner (CCL) or 0.01 m thick geosynthetic clay liner (GCL) under an applied head of 5 m. This comparison supports the use of a geomembrane as a liner in a tailings storage facility for situations where leakage is to be reduced.

In the field, the leakage under stresses similar to those applied in this study may be lower than reported in Table 3. The leakage could be impeded by the combined effect of (i) consolidation of tailings overlying the geomembrane; (ii) further deformation of the wrinkle; (iii) consolidation of tailings inside the wrinkle gap due to wrinkle deformation and (iv) higher resistance to flow due to the increased tailings thickness compared to the limited thickness of tailings placed in this study.

4.3. Long term performance of the geomembrane

With such large wrinkle deformations and all remaining gaps beneath the wrinkle filled with tailings, the effect of having a wrinkle with a hole on leakage may in fact be of lesser concern than having the same wrinkle with a hole in a landfill type application. There may, however, be a concern regarding long-term stress cracking at the locations where high curvatures were introduced on the wrinkle. Any strain induced cracking along these locations will increase leakage. More research is needed into this aspect.

5. CONCLUSIONS

Results from experiments involving wrinkles in four different geomembranes (1 and 2 mm thick LLDPE and HDPE) below a saturated tailings backfill were reported for a range of stress conditions. For the specific conditions and materials examined, it is concluded that

(1) Wrinkle deformations depended on the stiffness of the geomembrane and applied stresses. The 1 mm thick LLDPE and HDPE geomembrane wrinkles deformed to an extent that the gap beneath the wrinkle was eliminated, with both inner sides of the wrinkle physically coming into contact at 250 kPa. For 2 mm thick HDPE and LLDPE geomembrane wrinkles, the initial gap beneath the wrinkle was reduced in both height and width but remained up to the maximum applied total stress of 1000 kPa.

(2) The shape of the deformed geomembrane wrinkle was controlled by geomembrane stiffness and the presence of a hole in the wrinkle prior to placement of tailings slurry. Wrinkles in the 1 mm thick geomembrane without any hole deformed to a much narrower wrinkle, giving a near vertical projection with high curvatures at the wrinkle crest and base. A 2 mm thick geomembrane wrinkle without any hole reduced in both height and width to form a single smaller wrinkle. For wrinkles with a hole present prior to tailings placement, the final wrinkle shape was dependent on the extent to which the gap beneath the wrinkle was filled with tailings. The 1 mm thick geomembrane wrinkle experienced non-symmetrical deformation, with the wrinkle crest shifting towards the side without a hole. The stiffer 2 mm thick LLDPE geomembrane wrinkle was partially filled with tailings, and the wrinkle surface contained multiple locations with high curvature.

(3) The 2 mm thick HDPE geomembrane wrinkle below saturated tailings experienced a larger lateral deformation than that reported for a less stiff 1.5 mm thick HDPE geomembrane wrinkle below a gravel backfill under the same applied total stress.

(4) Leakage through a hole placed at the bottom of the wrinkle increased with an increase in total stress and pore pressure, whereas for cases with a hole placed on top side of the wrinkle, leakage decreased with an increase in total stress and pore pressure. Leakage for the case with a hole at the bottom of the wrinkle increased from 2.3 liters per day (lpd) to 7.6 lpd with an increase in total stress and pore pressure from total stress $p = 250$ kPa, pore pressure $u = 200$ kPa to $p = 1000$ kPa, $u = 500$ kPa. Leakage through a hole placed on top side of the wrinkle–irrespective of the time of hole formation–decreased from 8.5 lpd to 2.5 lpd with an increase in total stress and pore pressure from $p = 250$ kPa, $u = 200$ kPa to $p = 1000$ kPa, $u = 500$ kPa.

The leakage inferred from these cases would appear to be quite small for a reasonable number of holes with a wrinkle, although more research is needed to quantify additional cases.

ACKNOWLEDGEMENTS

This work was funded by the Natural Sciences and Engineering Research Council of Canada through a Collaborative Research and Development Grant in partnership with Klohn Crippen Berger Ltd. The value of discussions and the assistance and advice of H. McLeod is very gratefully acknowledged. The apparatus was developed with funding from the Canada Foundation for Innovation and the Ontario government.

NOTATION

Basic SI units are given in parentheses.

- C_c coefficient of curvature (dimensionless)
- C_u coefficient of uniformity (dimensionless)
- d_{10} particle diameter at which 10% of the sample mass is less than (m)
- d_{50} particle diameter at which 50% of the sample mass is less than (m)
- H height of a wrinkle (m)
- h head (m)
- k hydraulic conductivity/permeability (m/s)
- p total applied vertical stress (Pa)
- p' effective stress generated due to the difference between applied vertical stress and pore pressure (Pa)
- u applied pore pressure (Pa)
- W width of a wrinkle (m)

θ geomembrane-clay liner interface transmissivity (m^2/s)
κ stiffness index (N/m)
Ω relative tensile stiffness (dimensionless)

ABBREVIATIONS

CCL compacted clay liner
CQA construction quality assurance
GCD geocomposite drain
GCL geosynthetic clay liner
GMB geomembrane
HDPE high-density polyethylene
LLDPE linear low-density polyethylene
lpd liters per day
lpdh liters per day per hectare
MSW municipal solid waste

REFERENCES

Abdelaal, F. B., Rowe, R. K., Smith, M., Brachman, R. W. I. & Thiel, R. (2012). Antioxidant depletion from HDPE and LLDPE geomembranes without HALS in an extremely low pH solution. *The 2nd Pan American Geosynthetics Conference and Exhibition, GeoAmericas 2012*, Lima, Peru, CD-ROM.

Abdelaal, F. B., Rowe, R. K. & Brachman, R. W. I. (2013). Brittle rupture of an aged HDPE geomembrane at local gravel indentations under simulated field conditions. *Geosynthetics International*, **21**, No. 1, 1–23.

ASTM D6693/D6693M Standard test method for determining tensile properties of nonreinforced polyethylene and nonreinforced flexible polypropylene geomembranes. ASTM International, West Conshohocken, PA, USA.

Brachman, R. W. I. & Gudina, S. (2008). Geomembrane strains and wrinkle deformations in a GM/GCL composite liner. *Geotextiles and Geomembranes*, **26**, No. 6, 488–497.

Brachman, R. W. I., Joshi, P., Rowe, R. K. & Gudina, S. (2011). Physical response of geomembrane wrinkles near GCL overlaps. *Geo-Frontiers 2011*, Dallas, ASCE, Reston, VA, USA, pp. 1152–1161.

Brachman, R. W. I., Rowe, R. K. & Irfan, H. (2014). Short-term local tensile strains in HDPE heap leach geomembranes from coarse overliner materials. *ASCE Journal of Geotechnical and Geoenvironmental Engineering*, **140**, No. 5, 04014011-1–04014011-8.

Chappel, M. J., Brachman, R. W. I., Take, W. A. & Rowe, R. K. (2012a). Large-scale quantification of wrinkles in a smooth black HDPE geomembrane. *Journal of Geotechnical and Geoenvironmental Engineering*, **138**, No. 6, 671–679.

Chappel, M. J., Rowe, R. K., Brachman, R. W. I. & Take, W. A. (2012b). A comparison of geomembrane wrinkles for nine field cases. *Geosynthetics International*, **19**, No. 6, 453–469.

Colucci, P. & Lavagnolo, M. C. (1995). Three years field experience in electrical control of synthetic landfill liners. *Proc. 5th International Landfill Symposium, S. Margherita di Pula*, Cagliari, Italy (Christensen T. H., Cossu R. and Stegmann R. (eds)). CISA, Environmental sannitary engineering, Cagliari, Italy, pp. 437–452.

Dickinson, S. & Brachman, R. W. I. (2008). Assessment of alternative protection layers for a GM/GCL composite liner. *Canadian Geotechnical Journal*, **45**, No. 11, 1594–1610.

Ewais, A. M. R., Rowe, R. K., Brachman, R. W. I. & Arnepalli, D. N. (2014). Service-life of a HDPE GMB under simulated landfill conditions at 85°C. *ASCE Journal of Geotechnical and Geoenvironmental Engineering*, **140**, No. 11, 04014060.1-13.

Giroud, J. P. (1997). Equations for calculating the rate of liquid migration through composite liners due to geomembrane defects. *Geosynthetics International*, **4**, No. 3–4, 335–348.

Giroud, J. P. & Bonaparte, R. (1989a). Leakage through liners constructed with geomembranes – part I. *Geotextiles and Geomembranes*, **8**, No. 1, 27–67.

Giroud, J. P. & Bonaparte, R. (1989b). Leakage through liners constructed with geomembranes – part II. *Geotextiles and Geomembranes*, **8**, No. 2, 71–111.

Giroud, J. P. & Bonaparte, R. (2001). Geosynthetics in liquid-containing structures. *Chapter 26 of Geotechnical and Geoenvironmental Engineering Handbook* (Rowe R. K. (ed.)). Kluwer Academic Publishing, Norwell, MA, USA, pp. 789–824.

Gudina, S. & Brachman, R. W. I. (2006). Physical response of geomembrane wrinkles overlying compacted clay. *ASCE Journal of Geotechnical and Geoenvironmental Engineering*, **132**, No. 10, 1346–1353.

Pelte, T., Pierson, P. & Gourc, J. P. (1994). Thermal analysis of geomembrane exposed to solar radiation. *Geosynthetics International*, **1**, No. 1, 21–44.

Rowe, R. K. (1998). Geosynthetics and the minimization of contaminant migration through barrier systems beneath solid waste. *Keynote Lecture, Proc. 6th Int. Conf. on Geosynthetics*, Atlanta, GA, Industrial Fabrics Association International, St. Paul, MN, USA, vol. 1, pp. 27–103.

Rowe, R. K. (2012). Short and long-term leakage through composite liners, the 7th Arthur Casagrande Lecture. *Canadian Geotechnical Journal*, **49**, No. 2, 141–169.

Rowe, R. K., Quigley, R. M., Brachman, R. W. I. & Booker, J. R. (2004). *Barrier Systems for Waste Disposal Facilities*, Taylor & Francis Books Ltd. (E & FN Spon), London, UK.

Rowe, R. K., Chappel, M. J., Brachman, R. W. I. & Take, W. A. (2012). Field monitoring of geomembrane wrinkles at a composite liner test site. *Canadian Geotechnical Journal*, **49**, No. 10, 1196–1211.

Rowe, R. K., Brachman, R. W. I., Irfan, H., Smith, M. E. & Thiel, R. (2013). Effect of underliner on geomembrane strains in heap leach applications. *Geotextiles and Geomembranes*, **40**, 37–47.

Saathoff, F. & Sehrbrock, U. (1994). Indicators for selection of protection layers for geomembranes. In *Proceedings Fifth International Conference on Geotextiles, Geomembranes and Related Products* (Karunaratne G. P., Chew S. H. and Wong K. S. (eds)). International Geosynthetics Society, Singapore, pp. 1019–1022.

Soong, T. Y. & Koerner, R. M. (1998). Laboratory study of high density polyethylene geomembrane waves. *Proc., Int. Conf. on Geosynthetics, Industrial Fabrics Association International*, Industrial Fabrics Association International, St. Paul, MN, USA, vol. 1, pp. 301–306.

Stone, J. L. (1984). Leakage monitoring of the geomembrane for proton decay experiment. *Proc., Int. Conf. on Geomembranes, Industrial Fabrics Association International*, Industrial Fabrics Association International, St. Paul, MN, USA, vol. 2, pp. 475–480.

Take, W., Watson, E., Brachman, R. W. I. & Rowe, R. K. (2012). Thermal expansion and contraction of geomembrane liners subjected to solar exposure and backfilling. *J. Geotech. Geoenviron. Eng.*, **138**, No. 11, 1387–1397.

Terzaghi, K., Peck, R. B. & Mesri, G. (1996). *Soil Mechanics in Engineering Practice*, John Wiley & Sons, New York, NY, USA.

Tognon, A. R., Rowe, R. K. & Brachman, R. W. (1999). Evaluation of side wall friction for a buried pipe testing facility. *Geotextiles and Geomembranes*, **17**, No. 4, 193–212.

Tognon, A. R., Rowe, R. K. & Moore, I. D. (2000). Large scale testing of geomembrane protection layers. *ASCE Journal of Geotechnical and Geoenvironmental Engineering*, **126**, No. 12, 1194–1208.

The Editor welcomes discussion on all papers published in Geosynthetics International. Please email your contribution to discussion@geosynthetics-international.com